

ADVANCED EXPERIMENTAL METHODS FOR TURBULENT SHEAR FLOWS

Jerry Westerweel

Laboratory for Aero & Hydrodynamics,
Delft University of Technology
Mekelweg 2, 2628 CD Delft, the Netherlands
j.westerweel@tudelft.nl

ABSTRACT

Every experimental method provides a specific representation of the observed flow. Today, the use of *particle image velocimetry*, or PIV, is commonplace. The unique feature of PIV data is that it provides data of the instantaneous flow field and that it is capable of assessing the vorticity of the flow field. This paper provides an overview of recent advances in PIV and its application to turbulent shear flows.

INTRODUCTION

Most common fluids, like air and water, are homogeneous and optically transparent. It is therefore not possible to directly observe the fluid motion. An example is shown in Figure 1, which shows the view of a modern traveler in a jet airliner. The seemingly stationary scene does not reveal that only inches away air passes the window at speeds exceeding 800 km/h. Therefore it is necessary to take special approaches in order to make the fluid motion readily visible (Merzkirch 1987). Figure 2 shows a flow visualization of a cough by means of the *schlieren* method (Settles 2001). It is noted here that a picture such as shown in Figure 2 makes us readily aware of the extent of such a flow, which actually may change our social behavior (i.e., by placing a hand in front of one's mouth while coughing). Such flow visualizations provide qualitative insight in the behavior of fluid motion, which suits to classify the flow problem, e.g. whether the flow is stationary or turbulent, or whether or not flow separation occurs.

The introduction of inexpensive hardware for digital image processing, such as electronic image sensors and so-called *frame grabbers*, made it possible to perform a *quantitative* analysis of flow visualizations (Hesselink 1988). This approach has been ideally suited for the investigation of organized motion structures in turbulent shear flows (Cantwell



Figure 1: The view of the modern traveler.

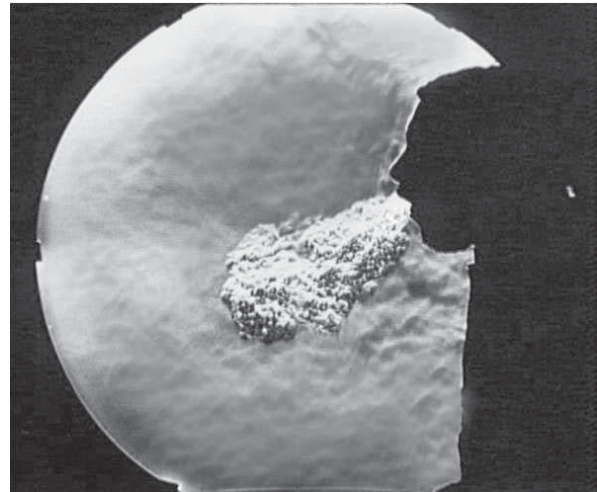


Figure 2: Schlieren visualization of a cough. (Courtesy of G.S. Settles, Penn. State Univ.)

1981; Robinson 1991). Such organized motion cannot be properly captured by means of single-point measurement techniques, such as *constant-temperature anemometry* (CTA) and *laser-Doppler anemometry* (LDA) (Goldstein 1996). Figure 3 shows a flow visualization, using the hydrogen-bubble wire method, and the velocity signal of a two-component LDA system of the flow in a turbulent boundary layer. While the flow visualization clearly the coherent fluid motion characteristic of a so-called *hair-pin vortex*, the LDA data represents the streamwise and wall-normal velocity of the flow as 'correlated noise'. The use of X-wire CTA probes and two-component LDA made it possible to directly measure the Reynolds stresses. This has allowed a significant advance in the description of turbulence and the validation of turbulence closure models. However, being essentially single-point measurements techniques, these methods are incapable to capture the instantaneous flow structure.

The development of *particle image velocimetry*, or PIV, made it possible to capture the instantaneous flow field by measuring the motion of small tracer particles in the fluid (Adrian 1991; Westerweel & Scarano 2007). A schematic of the basic elements and processes in a planar PIV system is shown in Figure 4. The tracer particles should be small enough so that they can accurately follow the fluid motion, but large enough to be visible. Typical particle diameters are 1-2 μm for air and 10-30 μm for liquids. The tracer particles are illuminated by a double-pulsed light source, usually a pulsed Nd:YAG laser. The laser beam is transformed into a thin light sheet that defines the measurement plane. The two exposures are recorded separately with a special dual-frame digital camera (which can record two successive frames with

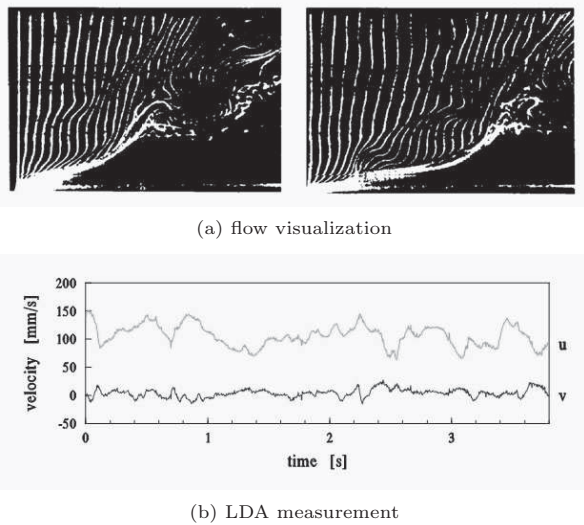


Figure 3: Turbulent boundary layer flow. (a) Flow visualization by means of the hydrogen-bubble wire method. From: Kim *et al.* (1971); (b) Measured streamwise and wall-normal velocity components (at 40 viscous wall units from the wall) by means of LDA. (Courtesy of: A. Schwarz-van Manen, Techn. Univ. Eindhoven).

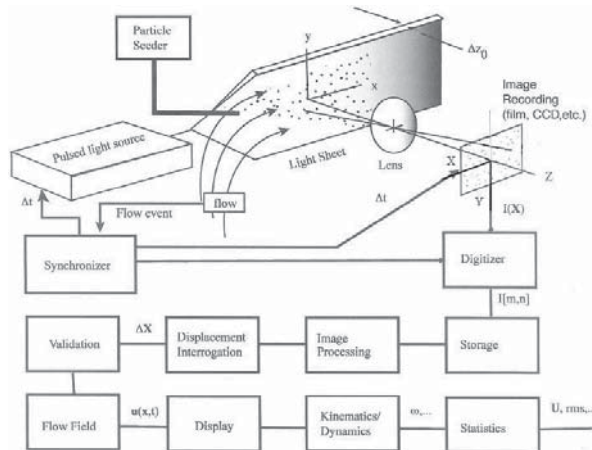


Figure 4: Elements and processes in a planar, two-dimensional particle image velocimeter system.

a time delay between 0.2 and 30 ms). The recorded image pairs are analyzed by means of a local correlation analysis, which yields the displacement of the particle-image pattern in each interrogation window. At low seeding densities it is common to match individual particle-image pairs, which is commonly referred to as *particle tracking velocimetry*, or PTV. This approach is ideally suited for the analysis of Lagrangian motion.

A typical PIV image pair can yield between 10^4 and 10^5 velocity measurements with an accuracy of 1%, representing a dynamic spatial and velocity ranges of the order of 10^2 (Adrian 1997). This corresponds to an uncertainty in the measured displacement of a tracer particle of about $4 \mu\text{m}$ under typical operating conditions.¹ The rate at which image pairs can be recorded depends on the specifications of

¹To appreciate this high level of accuracy, consider the thickness of a human hair (typically $60 \mu\text{m}$) at a distance of 30 cm (corresponding to the typical working distance for a PIV system).

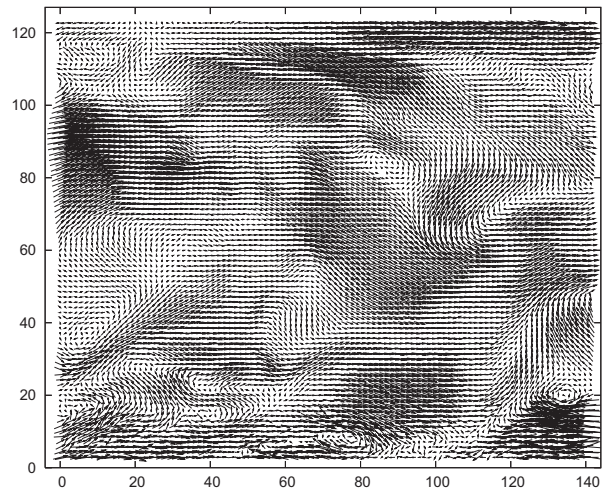


Figure 5: Result of a PIV measurement in a turbulent pipe flow at $Re = 5,300$. The plane of the light sheet is through the pipe centerline; top and bottom of the graph coincide with the pipe wall. The mean velocity profile has been subtracted. Dimensions are in mm. Details are given in a paper by Eggels *et al.* (1994).

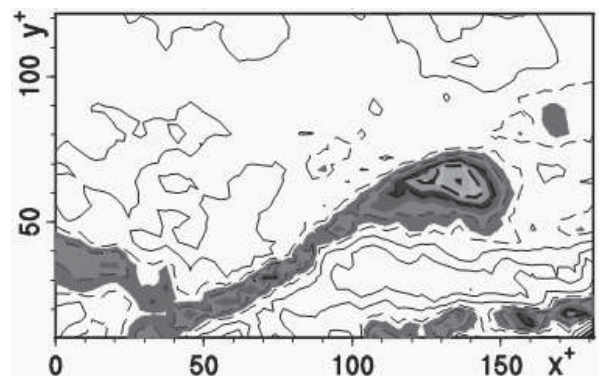


Figure 6: Out-of-plane component of the vorticity for a hair-pin vortex structure in the near-wall region of the turbulent pipe flow shown in Fig. 5; cf. Fig. 3a.

the laser system and digital camera(s); recording rates of 5×10^3 Hz are possible by combining a Nd:YLF laser and modern CMOS cameras. The number of frame pairs that can be recorded is between several hundred (for storage in RAM memory) to more than 10^4 frames (limited by hard-disk storage capacity). PIV is very versatile, and it can be applied over the full range of velocities, ranging from creeping flows to supersonic flows.

An example of the result of a PIV measurement in a plane through the centerline of a turbulent pipe flow is shown in Figure 5. Such measurements can reveal quantitative information on the hair-pin vortex structure shown in Figure 6; cf. Fig. 3a. This also illustrates the capability of PIV to assess the *vorticity* of the flow field.²

So, the principal advantage of the PIV method over other (single-point) measurement methods is the capability of assessing the instantaneous flow structure (*viz.*, vorticity field). The remainder of this paper summarizes how this has been utilized to obtain new insights in turbulent shear flows. In the following sections the modern implementations of PIV

²For planar PIV measurements only the out-of-plane component of the vorticity can be determined; this is simply referred to as the *vorticity*.

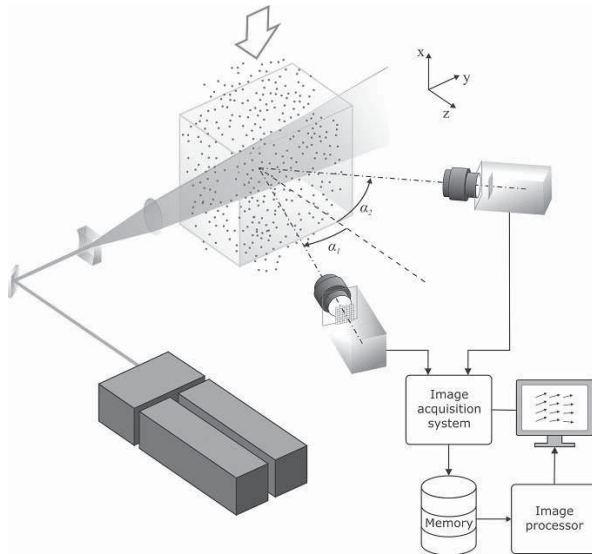


Figure 7: Typical configuration for a stereoscopic PIV system that can be used to determine all three velocity components in a planar cross section of the flow. From: Westerweel & Scarano (2007).

are described, and examples of results will be shown.

STEREOSCOPIC PIV

A single-camera PIV system only provides data on the in-plane velocity components (as shown in Fig. 5). Actually, such measurements are only yielding correct results when the out-of-plane component of the fluid velocity is small, otherwise the out-of-plane component contaminates the measurement of the in-plane components as the result of perspective effects. By using two cameras in a stereoscopic configuration, as shown in Figure 7, it is possible to reconstruct all three velocity components, including the out-of-plane component, from the small differences between the apparent particle-image displacements observed by each camera (Prasad 2000).

A stereoscopic PIV system was applied by van Doorne & Westerweel (2007) to study pipe flow. The plane of the light sheet was normal to the pipe axis. This approach was used to observe both transitional pipe flow and fully-developed turbulent pipe flow. In this configuration it was possible to observe the secondary fluid motion (i.e., normal to the axial velocity component) over the full cross section of the pipe. This provided the unique opportunity to look for experimental evidence of the existence of newly proposed traveling wave (TW) solutions of the Navier-Stokes equations for stationary pipe flow (Faisst & Eckhardt 2003; Wedin & Kerswell 2004). The comparison of measured flow patterns and the predicted TW patterns were reported by Hof & van Doorne *et al.* (2004); see also Figure 8.

Using a pair of high-speed cameras, it was possible to take time-resolved measurements and to reconstruct from successive measurements the quasi-instantaneous three-dimensional flow structure, i.e. effectively applying Taylor's hypothesis of *frozen turbulence*. This has been used to evaluate the flow structure of localized turbulence in transitional pipe flow, so-called *puffs* (Wynanski *et al.* 1975). An example of a puff measured by means of a high-speed stereoscopic PIV system is shown in Figure 9. It has been proposed that the life time of such localized disturbances would diverge at a critical Reynolds number (Faisst & Eckhardt 2004; Peixinho

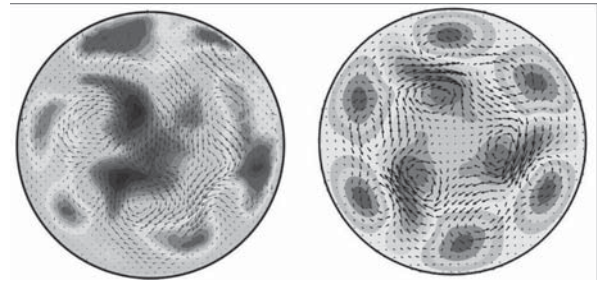


Figure 8: (left) Instantaneous cross-stream flow pattern (arrows) as observed with stereoscopic PIV in a turbulent puff in a pipe. Colors indicate deviation of the axial (or out-of-plane) component relative to laminar pipe flow, with red and blue indicating a positive and negative deviation respectively. (right) Numerical solution of a so-called *travelling wave* coherent flow state for pipe flow. From: Hof & van Doorne *et al.* (2004).

& Mullin 2006; Willis & Kerswell 2007) between 1780 and 2200. However, recent experimental findings indicate that the life time remains finite (Hof *et al.* 2006, 2008). Currently, new PIV measurements are in preparation that may reveal the decay process of puffs in detail.

MULTI-PLANE PIV

In the previous section, Taylor's hypothesis was used to reconstruct the (quasi-) instantaneous flow structure in a volumetric domain from a time series of planar PIV measurements. This can be avoided by using a scanning light sheet that quickly scans a given volume in multiple planes. This was first applied by Brücker (1996), and later Hori & Sakakibara (2004) applied a scanning-plane PIV system to measure the flow of a $Re = 1000$ submerged turbulent jet. This made it possible to obtain the instantaneous three-component vorticity field in a volumetric domain; see Figure 10. In this measurement the flow domain was recorded in 50 planes. Each full scan was completed in 0.22 s, which is about one-fifth of the integral time scale. Successive volumetric scans were obtained at 0.33 s intervals, which made it possible to retrieve the temporal evolution of the full vorticity field.

The scan of a full domain should be carried out before the flow undergoes significant changes. This implies that this approach would generally be limited to relatively low flow speeds when a large number of planes is involved. The temporal resolution can be significantly reduced when the number of planes is reduced. With two nearby planes it is possible to obtain the full deformation tensor in a planar cross section of the flow. This is sufficient to describe a turbulent flow with one or more (nearly) homogeneous directions, such as a turbulent boundary layer or turbulent channel flow. A description of a dual-plane stereoscopic PIV system is given by Kähler & Kompenhans (2000). Similar systems with different camera configurations and light-sheet configurations were applied by Ganapathisubramani *et al.* (2005) and Kim *et al.* (2006).

The combination of multiple planes can also be applied to combine the measurement of the velocity field with a scalar θ field using *laser-induced fluorescence*, or LIF. This provides information on turbulent scalar fluxes $u_i'\theta'$ (Webster *et al.* 2001; Fukushima *et al.* 2002). However, such data also allows a very different kind of analysis. The combined data can

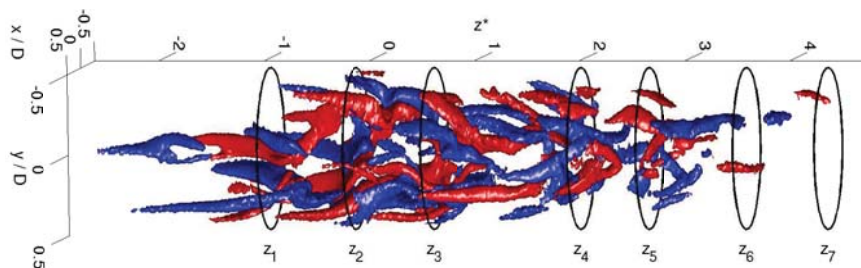


Figure 9: 3-D rendering of the iso-contours of streamwise vorticity ($\pm 3.5 \text{ s}^{-1}$) in a puff traveling downstream a pipe with $Re = 2000$. The puff travels from left to right. From: van Doorne & Westerweel (2009).

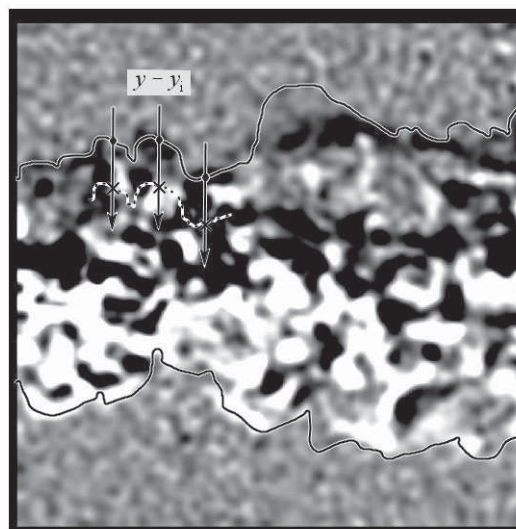
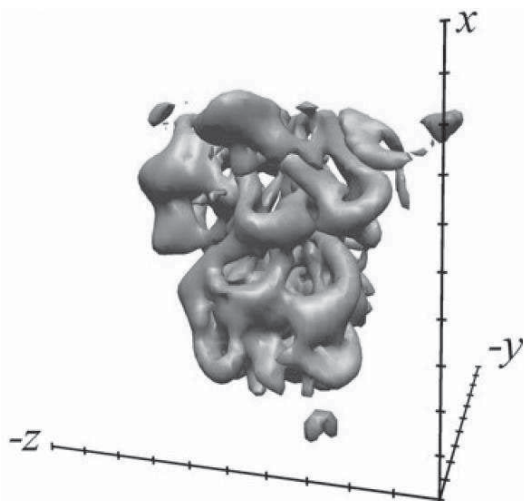


Figure 10: Surface of constant vorticity magnitude ($|\omega| = 2.5 \text{ s}^{-1}$). Result of a scanning laser PIV measurement of a $Re = 1000$ submerged jet. From: Hori & Sakakibara (2004).

be used to determine the conditional flow statistics relative to the turbulent/non-turbulent interface of a jet (Westerweel *et al.* 2002,2005). Here the jet fluid was marked with a fluorescent dye, and the scalar interface was used to define the turbulent/non-turbulent interface (Antonia 1981). Owing to the fact that PIV is capable of measuring the vorticity, it was thus possible for the first time to determine experimentally the existence of a thin shear layer at the turbulent/non-turbulent interface, and a corresponding finite jump in the axial momentum (Westerweel *et al.* 2005). This is characteristic for the laminar superlayer that separates the turbulent and non-turbulent flow regions (Corrsin and Kistler 1955; Townsend 1976). These combined PIV/LIF measurements provide quantitative results on the mechanics of these interface, and have provided new insights on the process of entrainment of ambient irrotational fluid into the turbulent flow region. It was thus found that small-scale turbulent motions, so-called ‘nibbling’, are the dominant entrainment process, rather than the large-scale vortical motions that can be readily observed in the results of Hori & Sakakibara (2004); see Fig. 10.

VOLUMETRIC METHODS

The use of multiple planes provides only a partial representation of the actual flow field. Hence, the development of volumetric methods that provide data on the full velocity field has been the ‘holy grail’ of experimental fluid dynamics.

holographic imaging Early approaches used holographic imaging to record a seeded flow volume. The most impres-

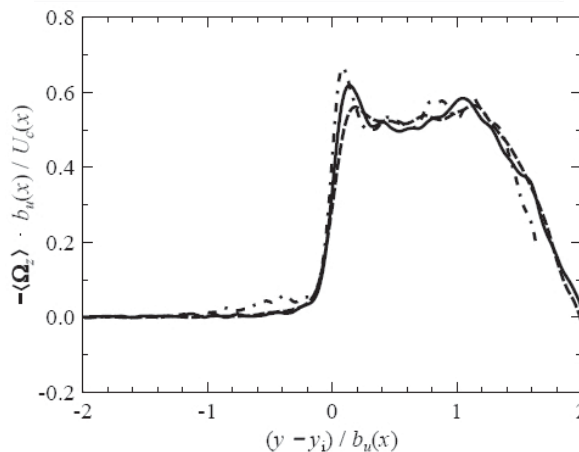


Figure 11: (top) Vorticity (i.e., the component normal to the measurement plane) and the jet envelope (continuous line). Conditional statistics are determined by averaging data at fixed distances relative to the envelope (indicated by the crosses and dashed line); (bottom) The mean conditional vorticity as a function of the distance from the interface at three different distances from the nozzle. From: Westerweel *et al.* (2005).

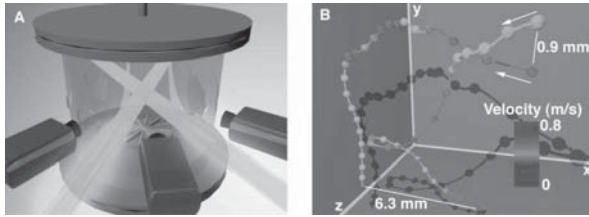


Figure 12: (a) Experimental configuration of three high-speed cameras to record the three-dimensional trajectories of $d_p = 25 \mu\text{m}$ tracer particles in a $50 \times 50 \times 50 \text{ mm}^3$ volume of an intense turbulent flow, illuminated by two expanded laser beams. (b) The trajectories of a particle pair. The small spheres indicate the measured positions at $74 \mu\text{s}$ intervals, with the larger spheres indicating every 30th frame. The color indicates the absolute velocity magnitude. From: Bourgoin *et al.* (2006).

sive result has been obtained by Barnhart *et al.* (1994). The main limitation of holographic methods has been the fact that for each recording a separate holographic plate needs to be used. This severely limits the number of realizations and makes it almost impossible to obtain information on the temporal evolution. Thanks to the availability of large-format electronic image sensors, such as CCD and CMOS arrays, it becomes possible to record holograms digitally, and to perform a computational reconstruction of the holograms, rather than optically reconstruction. Given the low spatial resolution of electronic image sensors (typically less than 100 line-pairs/mm) in comparison to holographic film (typically more than 2,000 line-pairs/mm), digital holography is limited to in-line configurations, which only allows the simultaneous observation of a few hundred particles. Especially at microscopic scales, where the image magnification is high and imaging methods are limited by the small focal depth, the use of digital holographic imaging is favorable. This was used by Sheng *et al.* (2008) to investigate the flow structures in the near-wall region of a turbulent boundary layer.

photogrammetry The main advantage of holographic imaging is that the depth-of-field is not bounded. Normal imaging is limited by a finite focal depth that strongly depends on the image magnification and the lens aperture. If the flow domain that has to be investigated is sufficiently shallow, it is possible to determine the positions of individual particles using multiple cameras; see Figure 12a. This is typically referred to as *photogrammetry* (Maas *et al.* 1993; Malik *et al.* 1993). Since individual tracer particles are observed, it is possible to reconstruct the Lagrangian trajectories of multiple particles in the flow. This approach has been used by Bourgoin *et al.* (2006) to determine the pair dispersion in isotropic turbulence. This also showed that fluid elements in a turbulent flow experience instantaneous accelerations in excess of $10^3 g$.

Photogrammetric particle tracking was applied by Holzner *et al.* (2008) to determine the flow field near the turbulent/non-turbulent interface of the propagating turbulent flow domain generated by an oscillating grid. These volumetric measurements confirmed and extended the earlier planar-domain results of Westerweel *et al.* (2005) for the turbulent/non-turbulent interface of a jet.

A simplified approach to a photogrammetric configuration was proposed by Willer & Gharib (1992), who apply a three-hole aperture. The defocused images then appear as three separate images arranged on the corners of trian-

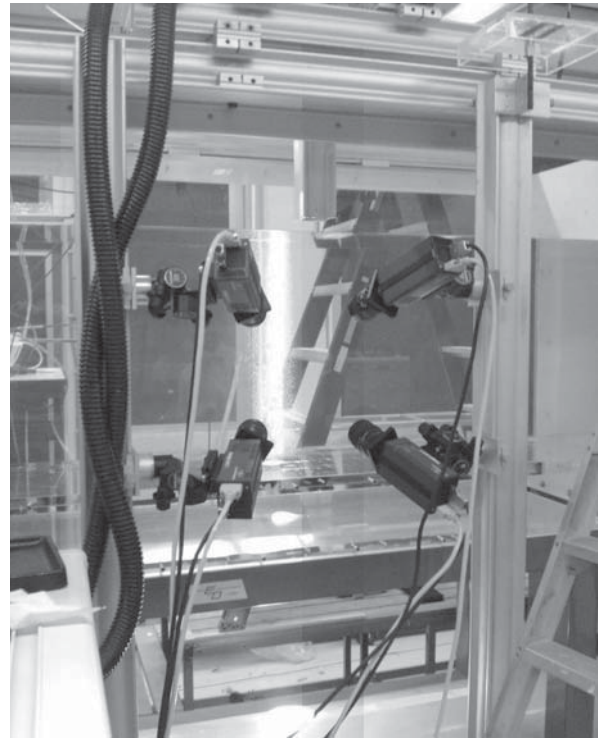


Figure 13: Camera arrangement for tomographic PIV applied in a $60 \times 60 \text{ cm}^2$ cross-section water tunnel.

gles. This makes it straightforward to detect and validate corresponding particle-image triples, where the area of the triangle is proportional to the axial distance of the particle. This approach has been refined by Pereira *et al.* (2000), using three separate cameras rather than a single camera with a three-hole aperture, thus improving the performance of the method.

tomographic PIV In photogrammetry the number of tracer particles that can be observed simultaneously is of the order a few hundred, and rarely exceeds 10^3 . This severely limits the spatial resolution of the measurement, which is especially a limitation for the investigation of turbulent shear flows. To avoid the detection of individual tracer particles, the volumetric distribution of point-like tracers can be reconstructed from multiple cameras by means of a tomographic reconstruction. This method was proposed and applied to turbulent shear flows by Elsinga *et al.* (2006).

A typical tomographic PIV set-up is shown in Figure 13. Each camera records the distribution of the light scattered by tracer particles in the measurement volume. Since a whole volume needs to be illuminated rather than a single thin plane, a high intensity light source is needed. To achieve a large depth-of-field, the aperture of the lens is reduced, which implies that only a small fraction of the scattered light is recorded. To have a sufficient signal, the particle diameter is usually increased with respect to applications of planar PIV. For flows in liquids (typically in water) the typical diameter of the tracer particles is $30\text{--}50 \mu\text{m}$, which provides a sufficient amount of scattered light.

The recorded intensity fields from the multiple cameras is back-projected into the measurement domain by means of a tomographic reconstruction method. The more cameras are used, the better the reliability of the reconstructed volumetric intensity field. The reconstruction of each particle using a finite number of views leads to the formation of so-called ‘ghost particles’, which can be considered as an artefact.

Typically four views provide a result with sufficient accuracy and reliability, while the improvement in using more than four views is marginal (Elsinga *et al.* 2006). To obtain a reliable and accurate reconstruction it is essential to have a proper alignment of the cameras. For this purpose a dedicated calibration procedure is required. Modern approaches are capable of calibrating the mapping of the images onto the measurement domain with a very high accuracy that allows the proper overlapping of the images of the tracer particles in the reconstruction. (It should be noted here that the back-projected particle images have a larger diameter than the actual tracer particles; this is the result of diffraction effects in the imaging of small particles using optics with a small aperture.)

The reconstructed volume typically has dimensions of $10^3 \times 10^3 \times 200$ voxels. The volume at two successive times (with a time delay Δt is sub-divided into small interrogation volumes, and for each interrogation volume a displacement (viz., velocity) is determined by computing the three-dimensional correlation. This is usually done in an iterative manner, where the corresponding interrogation volumes in two successive realizations is translated and deformed to maximize the number of particle-image pairs in the interrogation domain and minimize effects that decorrelate, such as particles that move across the boundary of the interrogation volume and variation of the displacement due to velocity gradients.

The typical measurement volume is $100 \times 100 \times 25$ mm³, which typically yields 10^5 data points (with overlapping interrogation domains) where the flow velocity is evaluated. This is two orders of magnitude higher than photogrammetric approaches. However, the reconstruction and interrogation can be computationally intensive.

As an example the results of a recent investigation by Scarano & Poelma (2009) using tomographic PIV of the turbulent flow behind a cylinder is shown in Figure 14. Since the total strain tensor is available, such data make it possible to readily assess the vortex stretching that occurs in turbulent flows. An example is shown in Figure 15.

CONCLUSION

This paper provides a brief overview of recent developments in optical diagnostics for the experimental investigation of turbulent shear flows and coherent flow structures. Planar systems are now commonplace, and provide accurate flow data using high-speed imaging systems. In recent years there has been a strong development in volumetric measurement systems that are capable of capturing the full deformation tensor. The spatial resolution of these methods is comparable to that of computational methods. However, the main advantage of experimental methods is that it can be applied to specific flow domains (for example, by only observing the near-wall flow region), whereas computational methods need to resolve the full flow domain and often rely on unrealistic boundary conditions.

The data that is provided by such measurements determine how we perceive and interpret the processes that occur in turbulent flows. As single-point methods, such as hot-wire anemometry and laser-Doppler anemometry, have fed the development of statistical models for turbulence, the modern optical methods that provide information on the instantaneous flow structure, and feed the development of models that are based on coherent fluid motions. Today, PIV is the only experimental method that is capable of measuring the

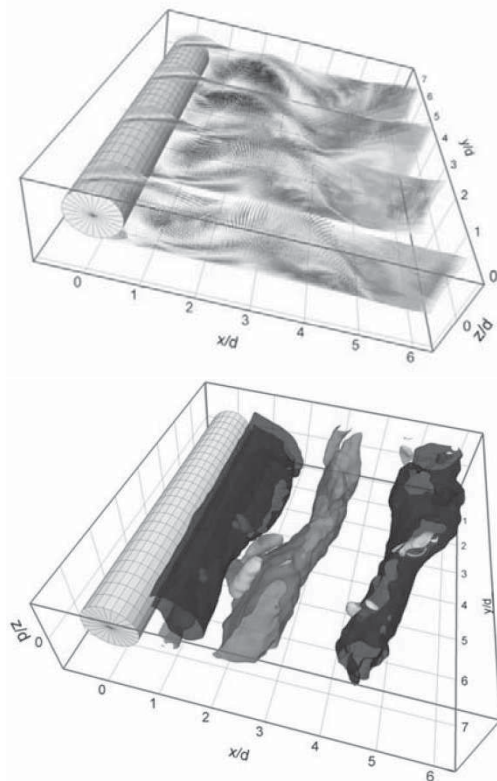


Figure 14: Instantaneous velocity and vorticity fields at $Re = 180$. Top: four planes of velocity vectors. Bottom: iso-surfaces of vorticity component. From: Scarano & Poelma (2009).

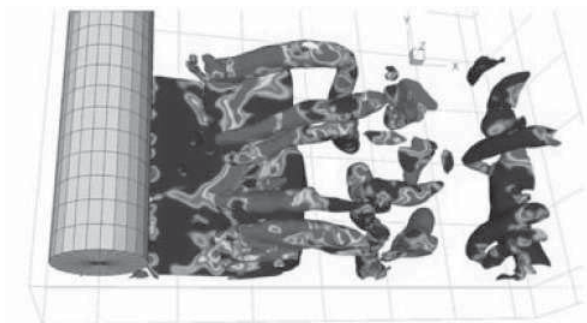


Figure 15: Flow behind a cylinder at $Re = 540$. Vorticity iso-contours color-coded with the vorticity stretching-tilting rate $\vec{\omega} \cdot \nabla \vec{u}$.

instantaneous spatial distribution of the vorticity.

It has been shown that modern experimental methods have been able to provide new insights in longstanding problems in turbulence, such as the transition to turbulence in pipe flow, the pair dispersion in turbulent mixing, and the entrainment process in free-shear flows.

Hence, modern experimental methods in turbulence go beyond tools that are needed for the validation of models, but actually may inspire the development of new concepts and approaches.

REFERENCES

Adrian, R.J., 1997, "Dynamic ranges of velocity and spatial resolution of particle image velocimetry" *Meas. Sci. Technol.* 8:1393-1398.

- Adrian, R.J., 1991, "Particle-imaging techniques for experimental fluid mechanics" *Annu. Rev. Fluid Mech.* 23:261-304.
- Antonia, R.A., 1981, "Conditional sampling in turbulence measurement" *Annu. Rev. Fluid Mech.* 13:131-156.
- Barnhart, D.H., Adrian, R.J. and Papen, G.C., 1994, "Phase-conjugate holographic system for high-resolution particle-image velocimetry" *Appl. Opt.* 33:7159-7170.
- Bourgoin, M., Ouellette, N.T., Xu, H., Berg, J. and Bodenschatz, E., 2006, "The role of pair dispersion in turbulent flow" *Science* 311:835-838.
- Brücker, Ch., 1996, "3-D Scanning-particle-image-velocimetry: technique and application to a spherical cap wake flow" *Appl. Sci. Res.* 56:157-179.
- Cantwell, B.J., 1981, "Organized motion in turbulent flow" *Annu. Rev. Fluid Mech.* 13:457-515.
- Corrsin, S. and Kistler, A.L., 1955, "Free-stream boundaries of turbulent flows" *NACA 1244* (Washington D.C.).
- van Doorne, C.W.H. and Westerweel, J., 2009, "The flow structure of a puff" *Phil. Trans. R. Soc. A* 367:489-507.
- Eggels, J.G.M., Unger, F., Weiss, M.H., Westerweel, J., Adrian, R.J., Friedrich, R. and Nieuwstadt, F.T.M., 1994, "Fully developed turbulent pipe flow: a comparison between direct numerical simulation and experiment" *J. Fluid Mech.* 268:175-209.
- Elsinga, G.E., Scarano, F., Wieneke, B. and van Oudheusden, B.W., 2006, "Tomographic particle image velocimetry" *Exp. Fluids* 41:933-947.
- Faisst, H. and Eckhardt, B., 2003, "Traveling waves in pipe flow" *Phys. Rev. Lett.* 91:224502.
- Faisst, H. and Eckhardt, B., 2004, "Sensitive dependence on initial conditions in transition to turbulence in pipe flow" *J. Fluid Mech.* 504:343-352.
- Fukushima, C., Aanen, L. and Westerweel, J., 2002, "Investigation of the mixing process in an axisymmetric turbulent jet using PIV and LIF" In: *Laser Techniques for Fluid Mechanics* (Eds. R.J. Adrian *et al.*), Springer (Berlin), pp. 339-356.
- Ganapathisubramani, B., Longmire, E.K., Marusic, I. and Pothos, S., 2005, "Dual-plane PIV technique to determine the complete velocity gradient tensor in a turbulent boundary layer" *Exp. Fluids* 39:222-231.
- Goldstein, R.J. (Ed.), 1996, *Fluid Mechanics Measurement* (2nd ed.), Taylor & Francis (Washington DC).
- Hesselink, L., 1988, "Digital image processing in flow visualization" *Annu. Rev. Fluid Mech.* 20:421-486.
- Hof, B., van Doorne, C.W.H., Westerweel, J., Nieuwstadt, F.T.M., Faisst, H., Eckhardt, B., Wedin, H., Kerswell, R.R. and Waleffe, F., 2004, "Experimental observation of nonlinear traveling waves in turbulent pipe flow" *Science* 305:1594-1598.
- Hof, B., Westerweel, J., Schneider, T.M. and Eckhardt, B., 2006, "Finite lifetime of turbulence in shear flows" *Nature* 443:59-62.
- Hof, B., de Lozar, A., Kuik, D.J. and Westerweel, J., 2008, "Repeller or attractor? Selecting the dynamical model for the onset of turbulence in pipe flow" *Phys. Rev. Lett.* 101:214501.
- Holzner, M., Liberzon, A., Nikitin, N., Lühti, B., Kinzelbach, W. and Tsinober, A., 2008, "A Lagrangian investigation of the small-scale features of turbulent entrainment through particle tracking and direct numerical simulation" *J. Fluid Mech.* 598:465-475.
- Hori, T. and Sakakibara, J., 2004, "High-speed scanning stereoscopic PIV for 3D vorticity measurement in liquids" *Meas. Sci. Technol.* 15:1067-1078.
- Kähler, C.J. and Kompenhans, J., 2000, "Fundamentals of multiple plane stereo particle image velocimetry" *Exp. Fluids* 29:S70-S77.
- Kim, H.T., Kline, S.J. and Reynolds, W.C., 1971, "The production of turbulence near a smooth wall in a turbulent boundary layer" *J. Fluid Mech.* 50:133-160.
- Kim, K.C., Yoon, S.Y., Kim, S.M., Chun, H.H. and Lee, I., 2006, "An orthogonal-plane PIV technique for the investigations of three-dimensional vortical structures in a turbulent boundary layer flow" *Exp. Fluids* 40:876-883.
- Maas, H.G., Gruen, A. and Papantoniou, D., 1993, "Particle tracking velocimetry in three-dimensional flows. Part 1. Photogrammetric determination of particle coordinates" *Exp. Fluids* 15:133-146.
- Malik, N.A., Dracos, Th. and Papantoniou, D.A., 1993, "Particle tracking velocimetry in three-dimensional flows — Part 2: particle tracking" *Exp. Fluids* 15:279-294.
- Merzkirch, W., 1987, *Flow Visualization* (2nd ed.), Academic Press (Orlando).
- Peixinho, J. and Mullin, T., 2006, "Decay of turbulence in pipe flow" *Phys. Rev. Lett.* 96:094501.
- Pereira, F., Gharib, M., Dabiri, D. and Modarress, D., 2000, "Defocusing digital particle image velocimetry: a 3-component 3-dimensional DPIV measurement technique. Application to bubbly flows" *Exp. Fluids* S78-S84.
- Prasad, A.K., 2000, "Stereoscopic particle image velocimetry" *Exp. Fluids* 29:103-116.
- Robinson, S.K., 1991, "Coherent motions in the turbulent boundary layer" *Annu. Rev. Fluid Mech.* 23:601-639.
- Scarano, F. and Poelma, C., 2009, "Three-dimensional vorticity patterns of cylinder wakes" *Exp. Fluids* (online).
- Settles, G.S., 2001, *Schlieren and Shadowgraph Techniques*, Springer-Verlag (Berlin).
- Sheng, J., Malkiel, E. and Katz, J., 2008, "Using digital holographic microscopy for simultaneous measurements of 3D near wall velocity and wall shear stress in a turbulent boundary layer" *Exp. Fluids* 45:1023-1035.
- Townsend, A.A., 1976, *The Structure of Turbulent Shear Flow* (2nd Ed.), Cambridge University Press (Cambridge).
- Webster, D.R., Roberts, P.J.W. and Ra'ad, L., 2001, "Simultaneous DPTV/PLIF measurements of a turbulent jet" *Exp. Fluids* 30:65-72.
- Wedin, H. and Kerswell, R.R., 2004, "Exact coherent structures in pipe flow: travelling wave solutions" *J. Fluid Mech.* 508:333-371.
- Westerweel, J., Hofmann, T., Fukushima, C. and Hunt, J.C.R., 2002, "The turbulent/non-turbulent interface at the outer boundary of a self-similar turbulent jet" *Exp. Fluids* 33:873-878.
- Westerweel, J., Fukushima, C., Pedersen, J.M. and Hunt, J.C.R., 2005, "Mechanics of the turbulent/nonturbulent interface of a jet" *Phys. Rev. Lett.* 95:174501.
- Westerweel, J. and Scarano, F., 2007, "Particle image velocimetry" In: *Handbook of Experimental Fluid Mechanics* (Eds. C. Tropea *et al.*), Springer (Heidelberg).
- Willert, C.E. and Gharib, M., 1992, "Three-dimensional particle imaging with a single camera" *Exp. Fluids* 12:353-358.
- Willis, A.P. and Kerswell, R.R., 2007, "Critical behavior in the relaminarization of localized turbulence in pipe flow" *Phys. Rev. Lett.* 98:014501.
- Wynanski, I., Sokolov, M. and Friedman, D., 1975, "On transition in a pipe. Part 2. The equilibrium puff" *J. Fluid Mech.* 69:283-304.